APPLIED PHYSICS REVIEWS—FOCUSED REVIEW

Wide band gap ferromagnetic semiconductors and oxides

S. J. Pearton,[a] C. R. Abernathy, M. E. Overberg, G. T. Thaler, and D. P. Norton
Department of Materials Science and Engineering, University of Florida, Gainesville, Florida 32611

N. Theodoropoulou and A. F. Hebard
Department of Physics, University of Florida, Gainesville, Florida 32611

Y. D. Park
Center for Strongly Correlated Materials Research, Seoul National University, Seoul 151-747, Korea

F. Ren and J. Kim
Department of Chemical Engineering, University of Florida, Gainesville, Florida 32611

L. A. Boatner
Solid State Division, Oak Ridge National Laboratory, Oak Ridge, Tennessee 37813

(Received 7 March 2002; accepted 3 May 2002)

Recent advances in the theory and experimental realization of ferromagnetic semiconductors give hope that a new generation of microelectronic devices based on the spin degree of freedom of the electron can be developed. This review focuses primarily on promising candidate materials (such as GaN, GaP and ZnO) in which there is already a technology base and a fairly good understanding of the basic electrical and optical properties. The introduction of Mn into these and other materials under the right conditions is found to produce ferromagnetism near or above room temperature. There are a number of other potential dopant ions that could be employed (such as Fe, Ni, Co, Cr) as suggested by theory [see, for example, Sato and Katayama-Yoshida, Jpn. J. Appl. Phys., Part 2 **39**, L555 (2000)]. Growth of these ferromagnetic materials by thin film techniques, such as molecular beam epitaxy or pulsed laser deposition, provides excellent control of the dopant concentration and the ability to grow single-phase layers. The mechanism for the observed magnetic behavior is complex and appears to depend on a number of factors, including Mn–Mn spacing, and carrier density and type. For example, in a simple Ruderman–Kittel–Kasuya–Yosida carrier-mediated exchange mechanism, the free-carrier/Mn ion interaction can be either ferromagnetic or antiferromagnetic depending on the separation of the Mn ions. Potential applications for ferromagnetic semiconductors and oxides include electrically controlled magnetic sensors and actuators, high-density ultralow-power memory and logic, spin-polarized light emitters for optical encoding, advanced optical switches and modulators and devices with integrated magnetic, electronic and optical functionality.
[DOI: 10.1063/1.1517164]

TABLE OF CONTENTS

[a]Electronic mail: spear@mse.ufl.edu

I. INTRODUCTION

There is currently a lot of interest in the science and potential technological applications of spin-transport electronics (or spintronics), in which the spin of charge carriers (electrons or holes) is exploited to provide new functionality for microelectronic devices.[1–23] The phenomena of giant magnetoresistance and tunneling magnetoresistance have been exploited in all-metal or metal–insulator–metal magnetic systems for read/write heads in computer hard drives, magnetic sensors and magnetic random access memories. The reader is referred to past reviews on these topics.[2,9,16,24–28] The development of magnetic semiconductors with practical ordering temperatures could lead to new classes of device and circuits, including spin transistors, ultradense nonvolatile semiconductor memory and optical emitters with polarized output.

Most of the past attention on ferromagnetic semiconductors has focused on the (Ga,Mn)As (Refs. 2 and 29–52) and (In,Mn)As (Refs. 53–60) systems. In samples carefully grown single phase by molecular beam epitaxy (MBE), the highest Curie temperatures reported are ~110 K for (Ga,Mn)As (Ref. 30) and ~35 K for (In,Mn)As.[13] For ternary alloys such as $(In_{0.5}Ga_{0.5})_{0.93}Mn_{0.07}As$, the Curie temperature is also low ~110 K.[61] A tremendous amount of research on these materials systems has led to some surprising results, such as the very long spin lifetimes and coherence times in GaAs (Ref. 4) and the ability to achieve spin transfer through a heterointerface,[62–79] of either a semiconductor/semiconductor or metal semiconductor. One of the most effective methods for investigating spin-polarized transport is by monitoring the polarized electroluminescence output from a quantum-well light-emitting diode into which the spin current is injected. Quantum selection rules that relate the initial carrier spin polarization and the subsequent polarized optical output can provide a quantitative measure of the injection efficiency.[67,69–71]

There are a number of essential requirements for achieving practical spintronic devices in addition to the efficient electrical injection of spin-polarized carriers. These include the capability to transport the carriers with high transmission efficiency within the host semiconductor or conducting oxide, the capability to detect or collect the spin-polarized carriers and to be capable of controlling transport through external means such as biasing of a gate contact on a transistor structure. The observation of spin current-induced switching in magnetic heterostructures is an important step in realizing practical devices.[80] Nitta *et al.*[81] demonstrated that spin–orbit interaction in a semiconductor quantum well could be controlled by applying a gate voltage. These key aspects of spin injection, spin-dependent transport, manipulation and detection form the basis of current research and future technology. The use of read sensors based on metallic spin valves in disk drives for magnetic recording is already a $US100 billion per year industry. It should also be pointed out that spintronic effects are inherently tied to nanotechnology, because of the short (~1 nm) characteristic length of some of the magnetic interactions. Combined with the expected low power capability of spintronic devices, this should lead to extremely high packing densities for memory elements. A recent review of electronic spin injection, spin transport and spin detection technologies has recently been given by Buhrman[82] as part of a very detailed and comprehensive study of the status and trends of research into spin electronics in Japan, Europe and the U.S. The technical issues covered fabrication and characterization of magnetic nanostructures, magnetism and spin control in these structures, magneto-optical properties of semiconductors and magneto-electronics and devices.[83] The nontechnical issues covered included industry and academic cooperation and long-term research challenges. The panel findings are posted on the Web.[83]

The purpose of this review is to focus on a particular emerging aspect of spintronics, namely, recent developments in achieving practical magnetic ordering temperatures in technologically useful semiconductors, including wide band gap nitrides and oxides. While the progress in synthesizing and controlling the magnetic properties of III-arsenide semiconductors has been astounding, the reported Curie temperatures are too low to have significant practical impact. A key development that focused attention on wide band gap semiconductors as being the most promising for achieving high Curie temperatures was the work of Dietl *et al.*[84] They employed the original Zener model of ferromagnetism[85] to predict T_C values that exceeded room temperature for materials such as GaN and ZnO containing 5% of Mn and a high hole concentration (3.5×10^{20} cm^{-3}). Figure 1 shows a compilation of the predicted T_C values, together with classification of the materials (e.g., group IV semiconductors, etc.). Since the appearance of the Dietl *et al.*[84] paper, remarkable progress has been made on the realization of materials with T_C values at or above room temperature.

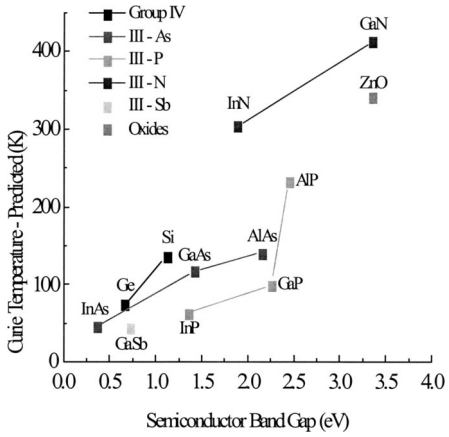

FIG. 1. Predicted Curie temperatures as a function of the band gap (after Ref. 84).

II. CANDIDATE MATERIALS

A. Semiconductors: Group III nitrides and phosphides

The wide band gap group III-nitrides (GaN, InN, AlN and their ternary and quaternary analogs) have been the focus of much attention in the last decade because of their application to blue/green/UV light-emitting diodes,[86] laser diodes,[87] solar-blind UV detectors[88] and high-power, high temperature electronics.[89,90] They can be grown in thin film form on lattice-mismatched substrates such as sapphire, SiC, Si and various oxides. This has been necessitated by the absence of commercially available large area bulk nitride substrates. The resulting high dislocation density in the nitride thin films (typically 10^8–10^{10} cm^{-2}, measured by transmission electron microscopy) has some deleterious effects on the reliability and produces excess leakage current in devices such as lasers. However, the commercial impact of nitride light emitters in allowing higher density data storage systems, visible displays (such as traffic signal lights) and potential use in indoor lighting applications using either white-light-emitting diodes (LEDs) (made by exciting appropriate phosphors with blue GaN LEDs) or color combining

TABLE I. Nitride parameters.

	Unit	GaN	AlN	InN
Crystal structure		Wurtzite	Wurtzite	Wurtzite
Density	g/cm	6.15	3.23	6.81
Transverse constant (C_t)	dyn/cm^2	4.42×10^{11}	4.42×10^{11}	4.42×10^{11}
Longitudinal constant (C_l)	dyn/cm^2	2.65×10^{11}	2.65×10^{11}	2.65×10^{11}
Transverse sound velocity	cm/s	2.68×10^5	3.70×10^5	2.55×10^5
Longitudinal sound velocity	cm/s	6.56×10^5	9.06×10^5	6.24×10^5
Static dielectric constant		8.9	8.5	15.3
High frequency dielectric constant		5.35	4.77	8.4
Energy gap (G valley)	eV	3.39	6.2	1.89
Electron effective mass (G valley)	m_e	0.20	0.48	0.11
Deformation potential	eV	8.3	9.5	7.1
Polar optical phonon energy	meV	91.2	99.2	89.0
Piezoelectric constant e_{14}	C/m^2	0.375	0.92	0.375
Piezoelectric constant e_{15}	C/m^2	⋯	-0.58	⋯
Piezoelectric constant e_{31}	C/m^2	⋯	$-0/48$	⋯
Piezoelectric constant e_{33}	C/m^2	⋯	1.55	⋯
Intervalley coupling coefficient	eV	91.2	99.2	89.0
Intervalley deformation potential	eV/cm	1×10^9	1×10^9	1×10^9
Lattice constant, a	Å	3.189	3.11	3.54
Lattice constant, c	Å	5.185	4.98	5.70
Electron mobility	cm^2/V s	1000 bulk 2000 (2D gas)	135	3200 bulk
Hole mobility	cm^2/V s	30	14	
Hole lifetime	ns	~7	⋯	⋯
Hole diffusion length (300 K)	m	$\sim0.8\times10^{-6}$	⋯	⋯
Nonparabolicity constant	$(\mathrm{eV})^{-1}$	0.189	⋯	0.419
Saturation velocity	cm/s	2.5×10^7	1.4×10^7	2.5×10^7
Peak velocity	cm/s	3.1×10^7	1.7×10^7	4.3×10^7
Peak velocity field	kV/cm	150 (455)	450	67
Breakdown field	V/cm	$>5\times10^6$		
Light hole mass	m_e	0.259 (454)	0.471	
Thermal conductivity	W/cm K	1.5	2	
Melting temperature	°C	>1700	3000	1100
Maximum electron concentration	cm^{-3}	10^{20}	2×10^{15}	3×10^{20}
Maximum hole concentration	cm^{-3}	$\sim10^{17}$	Usually resistive	N/A

the output of red, green and blue LEDs has been so great that rapid progress is also occurring for growth of GaN substrates and quasisubstrates that alleviate some of these problems.[91]

Table I shows some selected properties of binary nitrides.[92,93] For ternary compounds, $Al_xGa_{1-x}N$ and $In_xGa_{1-x}N$, the band gaps (Eg) can be expressed as a function of composition x, as follows[91]

$$Eg(Al_xGa_{1-x}N) = xEg(AlN) + (1-x)Eg(GaN) - bx(1-x),$$

$$Eg(In_xGa_{1-x}N) = xEg[InN] + (1-x)Eg(GaN) - bx(1-x),$$

where b is the bowing parameter whose exact value is still somewhat controversial, but ranges from 1 to 3.2 eV for InGaN and from -1 to $+1$ eV for AlGaN. Similarly, the electron effective masses are given by[91]

$$m^*(Al_xGa_{1-x}N) = 0.22 + 0.26x,$$

$$m^*(In_xGa_{1-x}N) = 0.22 - 0.11x.$$

One of the key entries in Table I is that for the maximum hole concentration reported in p-type material. In GaN, the most common acceptor dopant is Mg, with an ionization energy of $\sim$ 170 meV. At room temperature, therefore, only a few percent of the acceptors are ionized to provide holes. While the acceptor concentration can easily exceed 10^{19} cm^{-3}, the room temperature hole concentration is typically only $1-3\times10^{17}$ cm^{-3} in GaN(Mg). There are some indications that codoping both donors and acceptors (with a slight excess of the latter) into GaN can reduce self-compensation effects and produce higher hole concentrations.[94–97] An alternative method for increasing the hole concentration is the use of selectively Mg-doped AlGaN/GaN superlattices, in which there is transfer of free

TABLE II. Properties of phosphide and arsenide-based materials (after Ref. 103). The crystal structures are either sphalerite (Sph) or chalcopyrite (Chal).

	Crystal structure	Constant (Å)	Gap (eV)	Effective mass	Effective mass	Dielectric constant	Refractive index	Electron mobility ($cm^2/V\,s$)	Hole mobility ($cm^2/V\,s$)	Maximum doping n (cm^{-3})	Maximum doping p (cm^{-3})
AlP	Sph	5.4625	2.43*X*	0.13		9.8	3.0	80		$>10^{18}$	N/A
AlAs	Sph	5.6605	2.162.*X*	0.5	0.49	12.0		1,000	180	$>10^{18}$	$>10^{19}$
GaP	Sph	5.4506	2.26*X*	0.13	0.67	10	3.37	300	150	$>10^{19}$	$>10^{20}$
$ZnSiP_2$	Chal	*a* 5.400 *c* 10.441	2.96Γ	0.07				100		$>10^{18}$	N/A
$ZnSiAs_2$	Chal	*a* 5.606 *c* 10.890	2.12Γ		0.07				140	···	···
$ZnGeP_2$	Chal	*a* 5.465 *c* 10.771	2.34Γ		0.5				20	···	···
$ZnGeAs_2$	Chal	*a* 5.670 *c* 11.153	1.15Γ		0.4				23	···	···
$ZnSnP_2$	Chal	*a* 5.651 *c* 11.302	1.66Γ						55	···	···
$CdSiP_2$	Chal	*a* 5.678 *c* 10.431	2.45Γ	0.09				150		···	···
$CdSiAs_2$	Chal	*a* 5.884 *c* 10.882	1.55Γ						500	···	···
$CdGeP_2$	Chal	*a* 5.740 *c* 10.775	172Γ					100	25	···	···

holes from Mg acceptors in the AlGaN barriers to the GaN quantum wells.[98–100] In this case the effective hole density can be increased to $>10^{18}$ cm^{-3}.

In the case of AlN, the ionization level for Si donors is very deep, ~320 meV,[101] so that doping concentrations above 10^{19} cm^{-3} produce only $\sim 10^{15}$ cm^{-3} free electrons. The situation is even worse for *p*-type doping, where the C acceptor has an ionization level of approximately 500 meV. In this case only $\sim 10^{-7}$ of the acceptors would be ionized at room temperature in C-doped AlN.[97] For this reason, there have been few reliable reports of *p*-type AlN.

InN is generally *n* type due to the presence of native defects or unintentional donor incorporation. Films grown by MBE and related methods generally have very high free electron concentrations ($>10^{20}$ cm^{-3}), while material grown by reactive sputtering may have electron densities in the 10^{16} cm^{-3} range.[102] No one has yet reported achieving *p*-type doping of InN.

The ternary compounds $In_xGa_{1-x}N$ and $Al_xGa_{1-x}N$ can be readily doped *n* type, but only relatively low hole concentrations ($<10^{17}$ cm^{-3}) can be achieved at low InN or AlN mole fractions, respectively.

The relevance of these doping limitations comes from the fact that if the ferromagnetism in wide band semiconductors is carrier induced and its magnitude is proportional to the hole concentration (as in some models), then attention should be focused on these candidate materials which can be readily doped.

Table II shows some related properties of wide band gap phosphide and arsenide semiconductors.[103] The InGaAlP system, with its wide band gap binary (GaP, AlP) and ternary (InGaP, AlGaP, AlInP) components, is used for devices such as visible light-emitting diodes and laser diodes (the band gap ranges from 1.9 eV for $In_{0.49}Ga_{0.51}P$ which is lattice matched to GaAs substrates, to 2.3 eV for $(Al_xGa_{1-x})_{0.51}In_{0.49}P$ with $x=0.66$), heterojunction bipolar transistors and high electron mobility transistors. Binary compounds AlP and AlAs are unstable in air and oxidize rapidly unless covered with a capping layer. GaP is closely lattice matched to Si and introduces the possibility of integrating ferromagnetic semiconductors with existing Si microelectronics. Chalcopyrite materials are much less developed than the InGaAlP system and less is known about their doping properties and control of defects during growth.

B. Semiconducting oxides

In addition to nitrides, one can also consider transition-metal doped semiconducting oxides as potential spintronic materials. In fact, the theory by Dietl *et al.*[84] predicts room temperature ferromagnetism for Mn-doped *p*-type ZnO. ZnO is a direct band gap semiconductor with $E_g=3.35$ eV. The room temperature Hall mobility in ZnO single crystals is on the order of 200 $cm^2\,V^{-1}\,s^{-1}$.[104] ZnO normally has a hexagonal (wurtzite) crystal structure with $a=3.25$ Å and $c=5.12$ Å. Electron doping via defects originates from Zn interstitials in the ZnO lattice.[105] The intrinsic defect levels that lead to *n*-type doping lie approximately 0.05 eV below the conduction band. High electron carrier density can also be realized via group III substitutional doping. While *n*-type

TABLE III. Material properties for various semiconducting oxides taken from Refs. 180–182.

Compound	Crystal structure	Conductivity ($s\,cm^{-1}$)	Carrier type	Maximum mobility ($cm^2\,V^{-1}\,s^{-1}$)	Band gap (eV)	Maximum carrier concentration (cm^{-3})
$CuAlO_2$	Hexagonal	1	*P*	10	3.5	1.3×10^{17}
$CuGaO_2$	Hexagonal	0.063	*P*	0.25	3.6	1.7×10^{18}
$SrCu_2O_2$		0.05	*P*	0.5	3.3	6×10^{17}
$AgInO_2$	Hexagonal	6	*N*	0.5	4.2	2.7×10^{19}
ZnO	Hexagonal	20	*N*	200	3.2	1×10^{21}
In_2O_3	Cubic	10^4	*N*	30	3.75	1×10^{18}
Cd_2SnO_4	Orthogonal	10^4	*N*	40	2.7	
SnO_2	Tetragonal	10^4	*N*	10	3.6	8×10^{20}
TiO_2	Tetragonal		*N*	20–100	3.0	1×10^{19}
Cu_2O	Cubic		*P*	100	2.0	1×10^{17}

ZnO is easily realized via excess Zn or with Al, Ga, or In doping, *p*-type doping has proven difficult to achieve. Minegishi *et al.* reported the growth of *p*-type ZnO by simultaneous addition of NH_3 in hydrogen carrier gas with excess Zn.[106] However, the resistivity of these films was high with $\rho\sim100\ \Omega$ cm, suggesting that the mobile hole concentration was very low. Work by Rouleau *et al.*[107] on N-doped ZnO films shows that N incorporation does not necessary yield *p*-type behavior. In this case, nitrogen doping in epitaxial ZnO films was achieved using a rf nitrogen plasma source in conjunction with pulsed laser deposition. However, they showed no *p*-type behavior as determined by Hall measurements. *Ab initio* electronic band structure calculations for ZnO based on the local density approximation show that the Madelung energy decreases with *n*-type doping, consistent with experimental results for electron doping with Al, Ga, or In.[108] With N doping for holes, the Madelung energy increases, with significant localization of the N states. The theory does predict that codoping N with Ga to form an N–Ga–N complex can decrease the Madelung energy and delocalize the N states, thus facilitating hole doping. Using pulsed laser deposition, Joseph *et al.* have reported *p*-type behavior in ZnO thin films prepared by codoping Ga and N.[109] Electrically active N was achieved by passing N_2O gas through an electron cyclotron resonance plasma source. The authors reported low resistivity ($\rho=2\ \Omega$ cm, carrier density $\sim4\times10^{19}\ cm^{-3}$) *p*-type ZnO codoped with Ga and N in which the Ga concentration ranged from 0.1% to 5%. Unfortunately, these results have proven highly sensitive to processing conditions, and have been difficult to reproduce.

While there has been significant effort that has focused on nitrogen doping, almost no reported work exists for either As or P doping. However, *p*–*n* junction-like behavior was reported for *n*-type ZnO in which the surface was heavily doped with phosphorus.[110] Laser annealing a zinc phosphide-coated ZnO single crystal surface achieved the doping. A related result was reported for epitaxial ZnO films on GaAs subjected to annealing.[111] In this case, a *p*-type layer was produced at the GaAs/ZnO interface. Both of these reports are promising, but present several unresolved issues related to the solid solubility of the dopant (ionic radii of As, P much larger than that for O) and possible secondary phase formation in the doped region.

In addition to ZnO, one can also consider other semiconducting oxides. Table III shows the relevant properties for a number of oxide candidate materials. Both experimental and theoretical results suggest that carrier-mediated ferromagnetism in semiconductors is more favorable with *p*-type conductivity. This depends on the semiconductor and the magnetic species. For example, in EuX (where X=S, Se, etc.), the exchange is principally through the conduction band states even when they are not occupied.[23] Since the formation of *p*-type ZnO with high carrier density may prove challenging, it may be advantageous to explore the possibility of using oxide semiconductors that have been shown to exhibit *p*-type conduction with high carrier densities. Cu_2O is the only known binary *p*-type semiconducting oxide; it possesses a direct band gap of 2.0 eV and reasonably high room temperature hole mobility of $\sim100\ cm^2\,V^{-1}\,s^{-1}$. In Cu_2O, *p*-type conductivity is due to copper vacancies that introduce an acceptor level ~0.5 eV above the valence band. The structure is cubic, with $a=4.27$ Å.

In addition to Cu_2O, recent work in transparent conducting oxides has produced *p*-type behavior in semiconducting delafossite oxide materials.[111] For example, $CuAlO_2$ possesses the delafossite (hexagonal) crystal structure with $a=2.86$ Å and $c=11.31$ Å, and a band gap of ~3.5 eV. Carrier densities on the order of $10^{17}\ cm^{-3}$ with Hall mobility of $10\ cm^2\,V^{-1}\,s^{-1}$ have been measured. *P*-type conductivity is achieved via defects that introduce shallow acceptor levels. The $CuAlO_2$ phase has the advantage over Cu_2O of possessing two cation sites for possible magnetic substitution, including the Al^{+3} site that could yield an acceptor level with substitution of Mn^{+2}. Interestingly, it has been shown that $CuCrO_2$ forms in the delafossite structure and is a *p*-type semiconductor when doped with Ca.[112]

III. THEORY OF MAGNETIC SEMICONDUCTORS

There are a number of existing models for the observed magnetism in semiconductors and conducting oxides. The Dietl *et al.*[84] near-field model considers the ferromagnetism to be mediated by delocalized or weakly localized holes in *p*-type materials.[113] The magnetic Mn ion provides localized spin and acts as an acceptor in most III–V semiconductors so that it can also provide holes. This treatment assumes that the

Mn-doped III–V materials are charge transfer insulators and does not apply when *d*-shell electrons participate in charge transport. The spin–spin coupling is assumed to be a long-range interaction, allowing use of a mean-field approximation. The Curie temperature for a given material, Mn concentration and hole density is then determined by the competition between ferromagnetic and antiferromagnetic interactions. The model takes into account the anisotropy of the carrier-mediated exchange interaction related with the spin–orbit coupling in the host material. The T_C is proportional to the density of Mn ions and the hole density.

In the absence of carriers, the magnetization $M_O(H)$ is dependent on the Brillouin function B_s according to[84,113]

$$M_O(H) = g\mu_B S N_O X_{\text{eff}} B_s\left[\frac{g\mu_B H}{k_B(T+T_{\text{AF}})}\right],$$

where g is the degeneracy factor, μ_B is the Bohr magneton, S is the localized spin state, N_O is the concentration of cation sites, $N_O X_{\text{eff}}$ is the effective spin concentration, k_B is the Boltzmann constant and the antiferromagnetic (AF) temperature T_{AF} describes the sum of the exchange interactions to the Curie–Weiss temperature. In the presence of carriers, the magnetization is represented as[113]

$$M = \mu_G \mu_B S N_O X_{\text{eff}} B_s[g\mu_B(-\Delta F_C[M]/\Delta M + H)/k_B \times (T+T_{\text{AF}})],$$

where $F_C[M]$ is the hole contribution to the free-energy functional F, which is dependent on the magnetization of the localized spin. From this relation, T_C can be expressed[113–116]

$$T_C = X_{\text{eff}} N_O S(S+1)\beta^2 A_F P_S(T_C)/12k_B - T_{\text{AF}},$$

where β is the $p-d$ exchange integral, A_F is the Fermi liquid parameter and P_S is the total density of states. By substituting the appropriate materials parameters into this relation, the predicted values for T_C shown in Fig. 1 are obtained.

Recent Monte Carlo simulations of carrier-mediated ferromagnetism in semiconductors have also appeared[117,118] and have led to some differences from the mean-field approach. The latter usually overestimate the stability of ordered phases, which may lead to overly optimistic predictions for critical temperatures.[118] The kinetic-exchange model finds that collective spin-wave excitations are important and allows self-consistent accounting of spatial inhomogeneities, free-carrier exchange and free-carrier spin polarization.[119–121] Both the mean-field approach and kinetic-exchange model have been applied to a number of different phenomena in magnetic semiconductor systems including quantum wells,[122] interlayer coupling in superlattices,[121] temperature dependence of magnetization and heat capacity,[120] magnetic domain characteristics,[123] magnetic anisotropy,[124] and long-wavelength magnetic properties.[125]

It is certainly fair to say that the origin of ferromagnetism in wide band gap semiconductors is still not totally understood. Many aspects of the experimental data can be explained by the mean-field model [which is based on Ruderman–Kittel–Kasuya–Yosida (RKKY) interaction]. However, ferromagnetism has been observed in samples that have very low hole concentrations, in insulting material and more recently in *n*-type material. Recent models have taken into account these observations of ferromagnetism in nondegenerate samples, and included consideration of indirect exchange interactions caused by virtual electron excitations from magnetic impurity acceptors to the valence band[126] or the effects of positional disorder[127,128] which lead to unusual spin and charge transport properties and the shape of the magnetization curve. In some cases, positional disorder of the magnetic impurities is found to enhance the ferromagnetic transition temperature.[119] Self-consistent mean-field approaches have also been used to predict a Curie temperature enhancement in GaAs/GaMnAs digital alloy superlattices relative to the value in a bulk GaMnAs alloy with the same average Mn fraction,[129] and in δ-doped layers of Mn in a quantum well, due to improved confinement of holes.[130]

An alternative approach that uses local density functional calculations indicated that the magnetic impurities may form small nanosize clusters (just a few atoms in dimension) that produce the ferromagnetism observed.[131] This would be difficult to detect by most characterization techniques.

Additional studies have predicted which magnetic dopants should be most effective in GaN (e.g., V, Cr, Mn, Fe) without additional doping to produce carriers,[19,97,132] and chemical trends were identified.[19]

IV. EXPERIMENTAL RESULTS

Table IV gives a summary of the results showing ferromagnetism at or above room temperature. The materials include $CdMnGeP_2$,[133] (Ga,Mn)N,[134–137] (ZnO):Co,[138] (TiO_2):Co,[139,140] (GaMn)P:C,[141,142] $(Zn_{1-x}Mn_x)GeP_2$,[143,144] (Ga,Cr)N,[145] $ZnSnAs_2$,[146] and $ZnSiGeN_2$.[147] Note that not all of the materials are degenerately doped *p* type. In mean-field theories it is difficult to achieve ferromagnetism in *n*-type semiconductors due to their generally smaller $s-d$ interaction. In these types of theory, the $sp-d$ interactions are regarded as the effective magnetic field acting on the carriers, so that when spontaneous magnetization and holes are present, the resultant spin splitting in the valence band lowers the system energy.

Let us now examine in more detail the experimental results for some of the key wide band gap materials.

A. (Ga,Mn)P

Ferromagnetism above room temperature in (Ga,Mn)P has been reported for two different methods of Mn incorporation, namely, ion implantation[141] and doping during MBE growth.[141,142] The implantation process is efficient for rapidly screening whether particular combinations of magnetic dopants and host semiconductors are promising in terms of ferromagnetic properties. We have used implantation to introduce ions such as Mn, Fe and Ni into a variety of substrates, including GaN,[145,148–155] SiC,[153,156–158] and GaP.[141,159]

The temperature-dependent magnetization of a strongly *p*-type ($p \sim 10^{20}$), carbon-doped GaP sample implanted with ~ 6 at. % of Mn and then annealed at 700 °C, is shown in Fig. 2.[141] The diamagnetic contribution was subtracted from

TABLE IV. Compilation of semiconductors and oxides showing room temperature ferromagnetism.

Material	Band gap (eV)	Comments	Ordering temperature (K)	Reference
$Cd_{1-x}Mn_xGeP_2$	1.72	Solid-phase reaction of evaporated Mn	>300	133
(Ga,Mn)N	3.4	Mn incorporated by diff^n	228–370	134, 135
(Ga,Mn)N	3.4	Mn incorporated during MBE; *n* type	>300	136
(Ga,Mn)N	3.4	Mn incorporated during MBE	940[a]	137
(Ga,Cr)N	3.4	Cr incorporated during MBE	>400	145
(ZnO):Co	3.1–3.6	Co incorporated during PLD; ~15% Co	>300	138
(TiO_2):Co	3.1	Anatase; ~7% Co; PLD or O_2 MBE	>380	139, 140
(Ga, Mn)P:C	2.2	Mn incorporated by implant or MBE; p~10^{20} cm^{-3}	>330	141, 142
$(Zn_{1-x}Mn_x)GeP_2$	1.83–2.8	Sealed ampule growth; insulating; 5.6% Mn	312	143
(Zn, Mn)GeP_2	<2.8	Mn incorporated by diffusion	350	144
$ZnSnAs_2$	0.65	Bulk growth	329	146
$ZnSiGeN_2$	3.52	Mn-implanted epi	~300	147

[a]Extrapolated from measurements up to ~750 K.

the background. A Curie temperature (T_C) of ~270 K is indicated by the dashed vertical line, while the inset shows a ferromagnetic Curie temperature of 236 K.

Examples of hysteresis loops from the same samples are shown in Fig. 3. The hysteresis could be detected to 330 K. When Mn was implanted under the same conditions into *n*-GaP, the T_C was reduced to ~50 K.[141] No secondary phases (such as MnGa or MnP) or clusters were determined by transmission electron microscopy, x-ray diffraction or selected-area diffraction pattern analysis.

The Mn can also be incorporated during MBE growth of the (Ga,Mn)P.[142,160] The *p*-type doping level can be separately controlled by incorporating carbon from a CBr_4 source,[143] while P is obtained from thermal cracking of PH_3. Overberg *et al.*[142] have developed a phase diagram for epi growth of this materials system, as shown in Fig. 4. This can be used to tailor the magnetic properties of the (Ga,Mn)P. For samples grown at 600 °C with 9.4 at. % Mn, hysteresis is still detectable at 300 K, with a coercive field of ~39 Oe (Fig. 5).

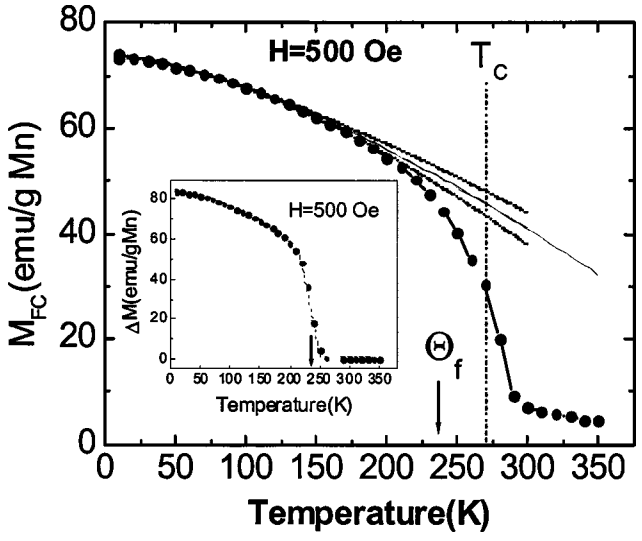

FIG. 2. Field-cooled magnetization of (Ga,Mn)P as a function of the temperature. The solid line shows a Bloch law dependence, while the dashed lines are 95% confidence bands. The vertical dashed line at $T_C = 270$ K is the field-independent inflection point and the vertical arrows in the main panel and inset mark the ferromagnetic Curie temperature Θ_f. The inset shows the temperature dependence of the difference in magnetization between field-cooled and zero field-cooled conditions (after Ref. 141).

B. (Ga,Mn)N

The initial work on this material involved either microcrystals synthesized by nitridization of pure metallic Ga in supercritical ammonia or bulk crystals grown in reactions of

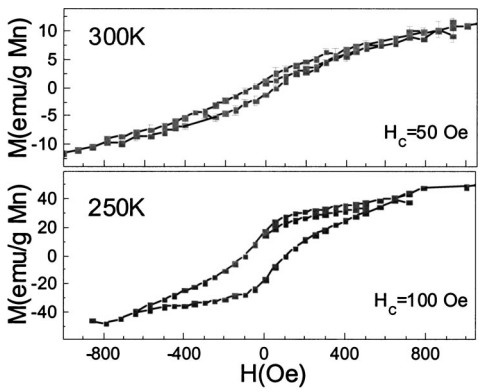

FIG. 3. Magnetization loops for (Ga,Mn)P at 300 (top) and 250 K (bottom) (after Ref. 141).

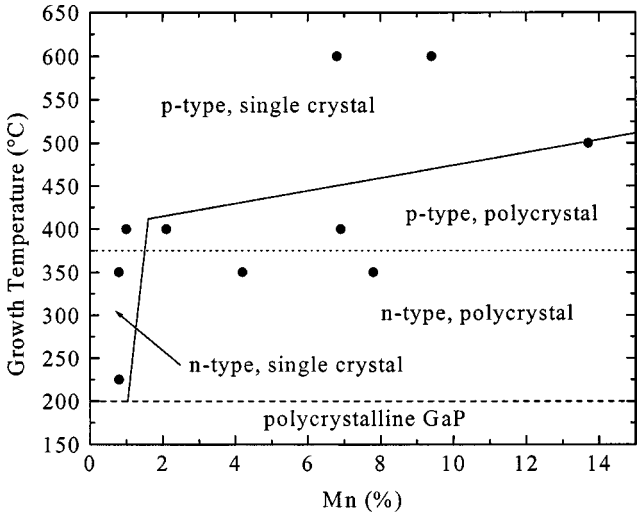

FIG. 4. Phase diagram for MBE-grown (Ga,Mn)P:C (after Ref. 142).

Ga/Mn alloys on GaN/Mn mixtures with ammonia at ~1200 °C.[161–164] These samples exhibit ferromagnetic properties over a broad range of Mn concentrations, as did some of the other early MBE-grown films.[165]

More recent reports on epi growth of (Ga,Mn)N have detailed a range of growth conditions producing single-phase material and the resulting magnetic properties.[136,142,166] In general, no second phases are found for Mn levels below ~10% for growth temperatures of ~750 °C. The (Ga,Mn)N retains *n*-type conductivity under these conditions. A powder diffraction scan of a sample with ~9 at. % Mn is shown in Fig. 6 (top). Only peaks from GaN and sapphire are visible. When the Mn concentration is increased significantly, peaks from tetragonal $Mn_{0.6}Ga_{0.4}$ become visible, as seen in Fig. 6 (bottom).

Since the predominant secondary phase that forms in bulk (Ga,Mn)N was reported to be Mn_3N_2, we wanted to ascertain the stable Mn_xN_y phase most likely to form under MBE growth conditions. By growing only with Mn and N_2 fluxes, it was determined from powder x-ray diffraction (Fig. 7) that the thermodynamically stable Mn_xN_y phase at this

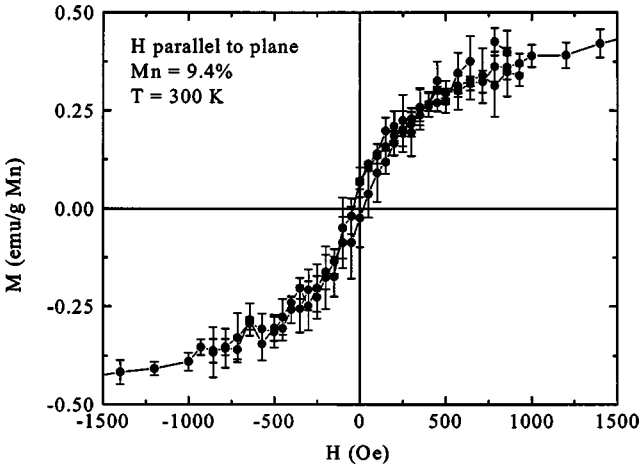

FIG. 5. Magnetization vs field for MBE-grown (Ga,Mn)P:C with 9.4 at. % Mn.

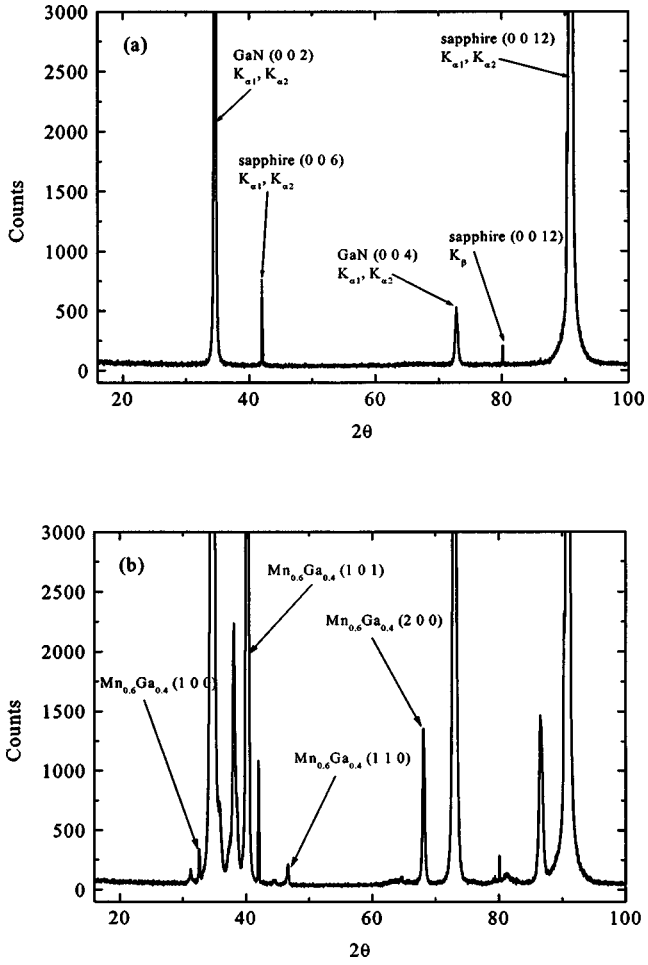

FIG. 6. X-ray diffraction scans from MBE-grown (Ga,Mn)N with ~9 at. % Mn (top) and ~43 at. % Mn (bottom).

growth temperature was Mn_4N. This phase has not been detected in any of our (Ga,Mn)N films.

In accordance with most of the theoretical predictions, magnetotransport data showed the anomalous Hall effect, negative magnetoresistance and magnetic resistance at temperatures that were dependent on the Mn concentration. For example, in films with very low (<1%) or very high

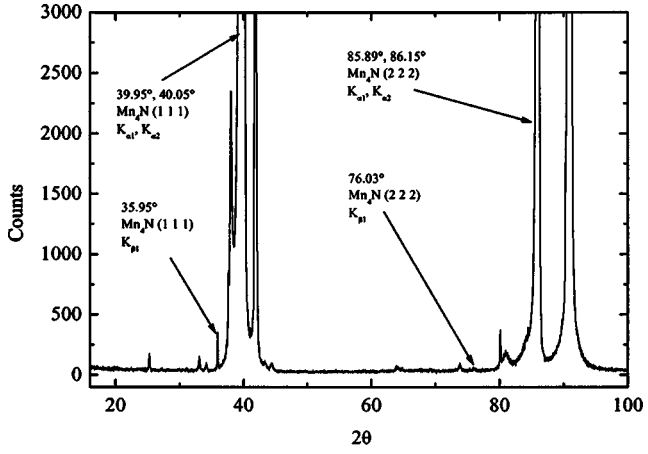

FIG. 7. X-ray diffraction scan from MBE-grown Mn_4N.

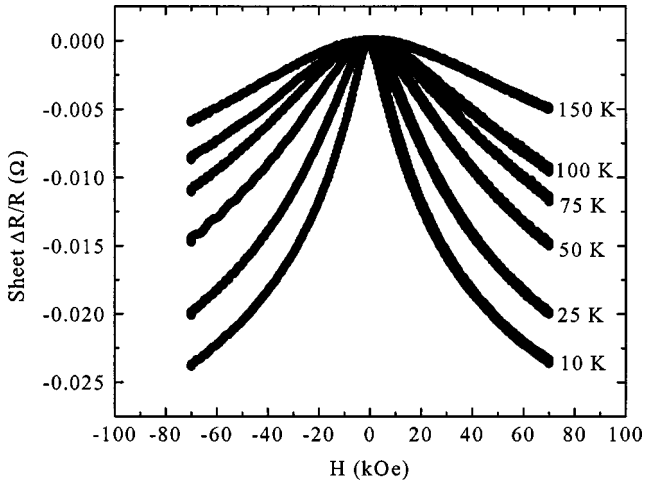

FIG. 8. Magnetotransport sheet resistance data from MBE-grown (Ga,Mn)N with ~7 at. % Mn. The magnetic field was applied perpendicular to the sample plane.

(~9%) Mn concentrations, the Curie temperatures were between 10 and 25 K.[166] An example is shown in Fig. 8 for an *n*-type (Ga,Mn)N sample with Mn of ~7%. The sheet resistance shows negative magnetoresistance below 150 K, with the anomalous Hall coefficient disappearing below 25 K. When the Mn concentration was decreased to 3 at. %, the (Ga,Mn)N showed the highest degree of ordering per Mn atom.[136] Figure 9(a) shows hysteresis present at 300 K, while the magnetization as a function of temperature is shown in Fig. 9(b). Data from samples with different Mn concentrations are shown in Fig. 9(c) that indicate ferromagnetic coupling, leading to a lower moment per Mn. Data from field-cooled and zero field-cooled conditions were further suggestive of room temperature magnetization.[136] The significance of these results is that there are many advantages from a device viewpoint to using *n*-type ferromagnetic semiconductors.

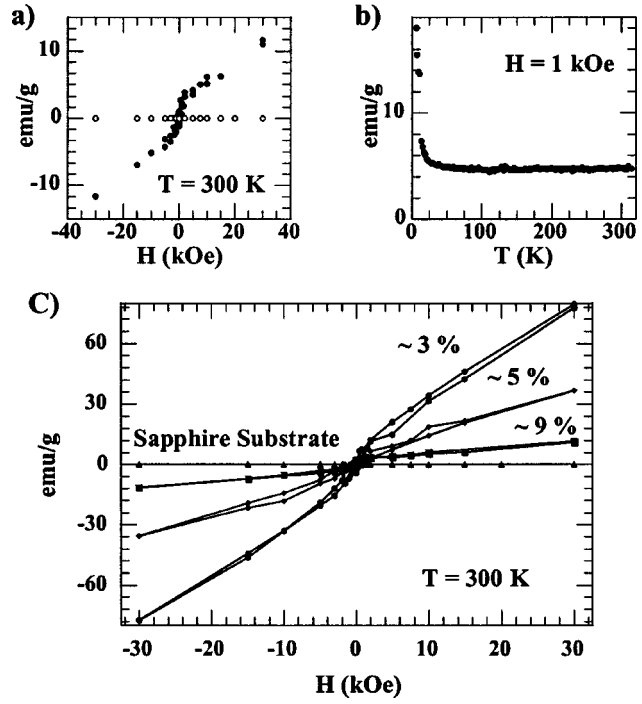

FIG. 9. (a) $B-H$ loops at 300 K from MBE-grown (Ga,Mn)N with ~9 at. % Mn (closed circles). The data from a sapphire substrate are shown by open circles. (b) Magnetization as a function of the temperature for the MBE-grown (Ga,Mn)N with ~9 at. % Mn. (c) $B-H$ loops at 300 K from MBE-grown (Ga,Mn)N with various Mn concentrations.

The local structure and effective chemical valency of Mn in MBE-grown (Ga,Mn)N samples were investigated by extended x-ray absorption fine structure (EXAFS) spectroscopy.[167] It was concluded that most of the Mn was incorporated substitutionally on the Ga sublattice with an effective valence close to +2 for samples with ~2 at. % Mn.[163] There was also evidence that a fraction (from 1% to 36%, depending on the growth conditions) of the total Mn concentration could be present as small Mn clusters.[167]

(Ga,Fe)N films grown by MBE have also been reported.[168] EXAFS data showed that the Fe was substitutional in Ga sites, with ferromagnetic ordering present below ~100 K for samples grown at ~380 °C.[168] Direct evidence of implanted Fe on substitutional Ga sites in GaN has come from emission channeling measurements.[169] It is possible that, with further optimization, GaN films doped with Fe, Ni and other impurities might also show room temperature ferromagnetism.

C. Transition metal doped oxides

In addition to Dietl *et al.*'s prediction, ferromagnetism in magnetically doped ZnO has been theoretically investigated by *ab initio* calculations based on local density approximation.[170] Again, the results suggest that ferromagnetic ordering of Mn is favored when mediated by hole doping. However, for V, Cr, Fe, Co, and Ni dopants, ferromagnetic ordering in ZnO is predicted to occur without the need of additional charge carriers. Recently, the magnetic properties of Ni-doped ZnO thin films were reported.[171] For films doped with 3–25 at. % Ni, ferromagnetism was observed at 2 K. Above 30 K, superparamagnetic behavior was observed. In all of these studies, the ZnO material was *n* type. We want to note that Fukumura *et al.* have shown that epitaxial thin films of Mn-doped ZnO can be obtained by pulsed laser deposition, with Mn substitution as high as 35% while maintaining the wurtzite structure.[172] This is well above the equilibrium solubility limit of ~13%, and illustrates the utility of low-temperature epitaxial growth in achieving metastable solubility in thin films. Codoping with Al resulted in *n*-type material with carrier concentration in excess of 10^{19} cm^{-3}. Large magnetoresistance was observed in the films, but no evidence of ferromagnetism was reported.

The theory of Dietl *et al.* predicting high temperature ferromagnetism for Mn-doped ZnO is specifically for *p*-type material. Experimental results reported in the literature for Mn-doped ZnO that is *n* type due to group III donor impurities are consistent with this prediction, and show no ferromagnetism. However, we recently obtained preliminary evidence of ferromagnetism in *n*-type ZnO, in which Mn and Sn serve as the transition metal and donor impurities, respectively. In these experiments, Mn ions were implanted at elevated temperature into Sn-doped ZnO single crystals. Mag-

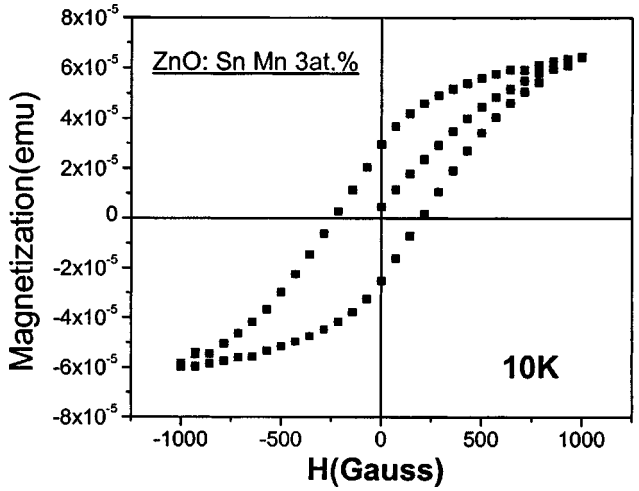

FIG. 10. B vs H curve for Mn-implanted ZnO:Sn single crystal, showing ferromagnetic behavior.

netization measurements showed clear hysteresis in the B vs H curves. Figure 10 shows the magnetization behavior at 10 K for a Sn-doped ZnO sample implanted with 3 at. % Mn, that clearly indicates ferromagnetism. More work is needed to determine the origin of ferromagnetism in these materials. If carrier-mediated mechanisms are responsible, one must explain why the behavior depends on the specific cation dopant specie chosen (Sn vs Al,Ga). Additional work is needed to address these issues.

It has recently been reported that anatase (TiO_2) doped with Co is a ferromagnetic semiconductor.[139,140] TiO_2 occurs in three distinct polymorphs, namely, rutile, anatase, and brookite. Rutile is the thermodynamically stable phase at high temperature, and is the most widely studied. Anatase is metastable, but can be stabilized in thin-film form. Undoped rutile is an anisotropic, tetragonal insulator ($a=4.59$ Å, $c=2.96$ Å) that possesses a band gap of ~ 3 eV. Anatase is also tetragonal ($a=3.78$ Å, $c=9.52$ Å) with a band gap of 3.2 eV.[173] At low temperatures, the permittivity of rutile is ~ 110 along the $a-b$ direction and ~ 240 along the c axis.[174] The static dielectric constant of anatase is 31.[175] TiO_2 can be made an n-type semiconductor with $n \sim 10^{19}/\text{cm}^3$ via cation substitution or by Ti interstitials.[176,177] Low temperature electron Hall mobility of the order of $30-100$ $\text{cm}^2/\text{V s}$ has been reported for rutile. Hall mobility of electron-doped anatase as high as 20 $\text{cm}^2/\text{V s}$ has been measured.

V. FUTURE DEVELOPMENTS AND CONCLUSIONS

The breakthroughs over the last few years in the understanding and control of spin-related effects in semiconductors have set the stage for a period of explosive growth in research and technological exploitation of spintronics. Most applications would require room temperature ferromagnetism and this is where materials such as (Ga,Mn)N, (Ga,Mn)P and (ZnO):Co may have a tremendous impact because their base materials can be produced by highly reproducible growth methods. In the case of the two semiconductors, there are already major technologies in place for visible light-emitting diodes. The expected advantages of spin devices include nonvolatility, higher integration densities, lower power operation and higher switching speeds. The ability to control the ferromagnetism through manipulation of the carrier density in gated semiconductor structures has great promise for integrated logic/memory/sensor chips.

Additional work is needed on the synthesis and control of carrier density in wide band gap semiconductor and conducing oxide thin films and on how the magnetic properties are related to the carrier type and density. Theoretical understanding of the origin of the ferromagnetism is progressing rapidly, but much work is needed to characterize the local environment around the Mn ions and the electrical properties of the Mn[178] and to have models that reproduce features of the experimental data.[179] This will require use of element-specific techniques such as transmission electron microscopy with Z contrast, EXAFS and various tunneling microscopies to correlate the lattice position and the presence of any nanoclusters with the resultant magnetic properties. Finally, it is imperative to fabricate a wide variety of spin-related device structures in order to identify the factors that limit their performance, which in turn will inevitably lead to improved contacts, cleaner interfaces and a clearer picture of spin-injection, control and transport issues.

ACKNOWLEDGMENTS

The authors are indebted to J. M. Poate and B. R. Appleton for their encouragement in writing this article and to Professor S. von Molnar for his comments. The work at the University of Florida was partially supported by the U.S. Army Research Office under Grant No. ARO DAAD 19-01-1-1701 (J. M. Zavada) and by the NSF under Grant Nos. DMR-0101856, DMR-0101438 and CTS-991173. The work at Seoul National University was partially supported by KOSEF and a Samsung Electronics endowment through CSCMR and by Seoul National University Research Foundation. Discussions with S. Arnason, P. Kumar, R. Bhatt, J. S. Lee, Z. G. Khim and D. Maslov are gratefully acknowledged.

[1] S. Das Sarma, J. Fabian, X. Hu, and Z. Zutic, IEEE Trans. Magn. **36**, 2821 (2000).
[2] G. A. Prinz, Science **282**, 1660 (1998).
[3] P. R. Hammar, B. R. Bennett, M. Y. Yang, and M. Johnson, Phys. Rev. Lett. **83**, 203 (1999).
[4] D. D. Awschalom and J. M. Kikkawa, Phys. Today **52**, 33 (1999).
[5] J. M. Kikkawa, I. P. Smorchkova, N. Samarth, and D. D. Awschalom, Science **277**, 1284 (1997).
[6] J. M. Kikkawa and D. D. Awschalom, Science **287**, 473 (2000).
[7] S. A. Wolf and D. Treger, IEEE Trans. Magn. **36**, 2748 (2000).
[8] J. Gregg, J. Magn. Magn. Mater. **175**, 1 (1997).
[9] M. Johnson, IEEE Spectrum **31**, 47 (1994).
[10] H. Ohno, Science **281**, 951 (1998).
[11] H. Ohno, J. Magn. Magn. Mater. **200**, 110 (1999).
[12] P. Ball, Nature (London) **404**, 918 (2000).
[13] H. Ohno, J. Vac. Sci. Technol. B **18**, 2039 (2000); H. Ohno, F. Matsukura, and Y. Ohno, Jap. Soc. Appl. Phys. Int. **5**, 4 (2002).
[14] T. M. Pekarek, B. C. Crooker, I. Miotkowski, and A. K. Ramdas, J. Appl. Phys. **83**, 6557 (1998).
[15] H. Ohno, D. Chibu, F. Matsukura, T. Omiya, E. Abe, T. Dietl, Y. Ohno, and K. Ohtani, Nature (London) **408**, 944 (2000).
[16] G. Prinz and K. Hathaway, Phys. Today **48**, 24 (1995).
[17] M. Tanaka, J. Cryst. Growth **201/202**, 660 (1999).

[18] T. Dietl, in *Handbook on Semiconductors*, edited by T. S. Moss (North-Holland, Amsterdam, 1994), Vol. 3B, p. 1251.
[19] K. Sato and H. Katayama-Yoshida, Jpn. J. Appl. Phys., Part 1 **40**, 4485 (2001).
[20] H. Ohno and F. Matsukura, Solid State Commun. **117**, 179 (2001).
[21] S. A. Wolf, D. D. Awschalom, R. A. Buhrman, J. M. Daughton, S. von Molnar, M. L. Roukes, A. Y. Chtchelkanova, and D. M. Treger, Science **294**, 1488 (2001).
[22] H. Ohno, H. Munekata, S. von Molnar, and L. L. Chang, J. Appl. Phys. **69**, 6103 (1991).
[23] F. Holtzberg, S. von Molnar, and J. M. D. Coey, *Handbook on Semiconductors*, edited by T. S. Moss (North-Holland, Amsterdam, 1980), p. 803.
[24] A. Fert, P. Grunberg, A. Barthelemy, F. Petroff, and W. Zinn, J. Magn. Magn. Mater. **140–144**, 1 (1995).
[25] *Ultra Thin Magnetic Structures*, edited by J. A. C. Bland and B. Heinrich (Springer, Berlin, 1994), Vols. I and II.
[26] C. H. Tsang, R. E. Fontana, Jr., T. Lin, D. E. Heim, B. A. Gurney, and M. L. Williams, IBM J. Res. Dev. **42**, 103 (1998).
[27] J. M. Daughton, P. Bade, M. Jenson, and M. Rahmati, IEEE Trans. Magn. **28**, 2488 (1992).
[28] S. S. P. Parkin, Phys. Rev. Lett. **71**, 1641 (1993).
[29] F. Matsukura, H. Ohno, A. Shen, and Y. Sugawara, Phys. Rev. B **57**, R2037 (1998).
[30] H. Ohno, A. Shen, F. Matsukura, A. Oiwa, A. Endo, S. Katsumoto, and Y. Iye, Appl. Phys. Lett. **69**, 363 (1996).
[31] R. Shioda, K. Ando, T. Hayashi, and M. Tanaka, Phys. Rev. B **58**, 1100 (1998).
[32] Y. Satoh, N. Inoue, Y. Nishikawa, and J. Yoshino, *Proceedings of the 3rd Symposium on Physics and Applications of Spin-Related Phenomena in Semiconductors, November 1997, Sendai, Japan*, edited by H. Ohno, J. Yoshino, and Y. Oka, (Jap. Soc. Appl. Phys., Tokyo) p. 23.
[33] T. Hayashi, M. Tanaka, T. Nishinaga, H. Shimoda, H. Tsuchiya, and Y. Otsuka, J. Cryst. Growth **175**, 1063 (1997).
[34] A. Van Esch *et al.*, Phys. Rev. B **56**, 13103 (1997).
[35] B. Beschoten, P. A. Crowell, I. Malajovich, D. D. Awschalom, F. Matsukura, A. Shen, and H. Ohno, Phys. Rev. Lett. **83**, 3073 (1999).
[36] M. Tanaka, J. Vac. Sci. Technol. B **16**, 2267 (1998).
[37] Y. Nagai, T. Kunimoto, K. Nagasaka, H. Nojiri, M. Motokawa, F. Matsukura, T. Dietl, and H. Ohno, Jpn. J. Appl. Phys., Part 1 **40**, 6231 (2001).
[38] J. Sadowski *et al.*, Appl. Phys. Lett. **78**, 3271 (2001).
[39] A. Shen, F. Matsukura, S. P. Guo, Y. Sugawara, H. Ohno, M. Tani, A. Abe, and H. C. Liu, J. Cryst. Growth **201/202**, 379 (1999).
[40] H. Shimizu, T. Hayashi, T. Nishinaga, and M. Tanaka, Appl. Phys. Lett. **74**, 398 (1999).
[41] B. Grandidier, J. P. Hys, C. Delerue, D. Stievenard, Y. Higo, and M. Tanaka, Appl. Phys. Lett. **77**, 4001 (2000).
[42] R. K. Kawakami, E. Johnson-Halperin, L. F. Chen, M. Hanson, N. Guebels, J. S. Speck, A. C. Gossard, and D. D. Awschalom, Appl. Phys. Lett. **77**, 2379 (2000).
[43] K. Ando, T. Hayashi, M. Tanaka, and A. Twardowski, J. Appl. Phys. **83**, 6548 (1998).
[44] D. Chiba, N. Akiba, F. Matsukura, Y. Ohno, and H. Ohno, Appl. Phys. Lett. **77**, 1873 (2000).
[45] H. Ohno, F. Matsukura, T. Owiya, and N. Akiba, J. Appl. Phys. **85**, 4277 (1999).
[46] T. Hayashi, M. Tanaka, T. Nishinaga, and H. Shimada, J. Appl. Phys. **81**, 4865 (1997).
[47] T. Hayashi, M. Tanaka, K. Seto, T. Nishinaga, and K. Ando, Appl. Phys. Lett. **71**, 1825 (1997).
[48] A. Twardowski, Mater. Sci. Eng., B **63**, 96 (1999).
[49] T. Hayashi, M. Tanaka, and A. Asamitsu, J. Appl. Phys. **87**, 4673 (2000).
[50] N. Akiba, D. Chiba, K. Natata, F. Matsukura, Y. Ohno, and H. Ohno, J. Appl. Phys. **87**, 6436 (2000).
[51] S. J. Potashnik, K. C. Ku, S. H. Chun, J. J. Berry, N. Samarth, and P. Schiffer, Appl. Phys. Lett. **79**, 1495 (2001).
[52] G. M. Schott, W. Faschinger, and L. W. Molenkanp, Appl. Phys. Lett. **79**, 1807 (2001).
[53] H. Munekata, H. Ohno, S. von Molnar, A. Segmuller, L. L. Chang, and L. Esaki, Phys. Rev. Lett. **63**, 1849 (1989).
[54] H. Akai, Phys. Rev. Lett. **81**, 3002 (1998).
[55] H. Ohno, H. Munekata, T. Penney, S. von Molnar, and L. L. Chang, Phys. Rev. Lett. **68**, 2664 (1992).
[56] H. Munekata, A. Zaslevsky, P. Fumagalli, and R. J. Gambino, Appl. Phys. Lett. **63**, 2929 (1993).
[57] S. Koshihara, A. Oiwa, M. Hirasawa, S. Katsumoto, Y. Iye, C. Urano, H. Takagi, and H. Munekata, Phys. Rev. Lett. **78**, 4617 (1997).
[58] Y. L. Soo, S. W. Huang, Z. H. Ming, Y. H. Kao, and H. Munekata, Phys. Rev. B **53**, 4905 (1996).
[59] A. Oiwa, T. Slupinski, and H. Munekata, Appl. Phys. Lett. **78**, 518 (2001).
[60] Y. Nishikawa, A. Tackeuchi, M. Yamaguchi, S. Muto, and O. Wada, IEEE J. Sel. Top. Quantum Electron. **2**, 661 (1996).
[61] T. Slupinski, H. Munekata, and A. Oiwa, Appl. Phys. Lett. **80**, 1592 (2002).
[62] I. Malajovich, J. M. Kikkawa, D. D. Awschalom, J. J. Berry, and N. Samarth, Phys. Rev. Lett. **84**, 1015 (2000).
[63] P. R. Hammar, B. R. Bennett, M. Y. Yang, and M. Johnson, J. Appl. Phys. **87**, 4665 (2000).
[64] A. Hirohata, Y. B. Xu, C. M. Guetler, and J. A. C. Bland, J. Appl. Phys. **87**, 4670 (2000).
[65] M. Johnson, J. Vac. Sci. Technol. A **16**, 1806 (1998).
[66] C. Gould, G. Schmidt, G. Richler, R. Fiederling, P. Grabs, and L. W. Molenkamp, Appl. Surf. Sci. **190**, 395 (2002).
[67] R. Fiederling, M. Kein, G. Reresche r, W. Ossan, G. Schmidt, A. Wang, and L. W. Molenkamp, Nature (London) **402**, 787 (1999).
[68] G. Borghs and J. De Boeck, Mater. Sci. Eng., B **84**, 75 (2001).
[69] Y. Ohno, D. K. Young, B. Bescholen, F. Matsukura, H. Ohno, and D. D. Awschalom, Nature (London) **402**, 790 (1999).
[70] B. T. Jonker, Y. D. Park, B. R. Bennett, H. D. Cheong, G. Kiseoglou, and A. Petrou, Phys. Rev. B **62**, 8180 (2000).
[71] Y. D. Park, B. T. Jonker, B. R. Bennett, G. Itskos, M. Furis, G. Kioseoglou, and A. Petrou, Appl. Phys. Lett. **77**, 3989 (2000).
[72] G. Schmidt, D. Ferrand, L. W. Molenkamp, A. T. Filip, and B. J. van Wees, Phys. Rev. B **62**, R4790 (2000).
[73] Y. Q. Jin, R. C. Shi, and S. J. Chou, IEEE Trans. Magn. **32**, 4707 (1996).
[74] C. M. Hu, J. Nitta, A. Jensen, J. B. Hansen, and H. Takayanagai, Phys. Rev. B **63**, 125333 (2001).
[75] F. G. Monzon, H. X. Tang, and M. L. Roukes, Phys. Rev. Lett. **84**, 5022 (2000).
[76] S. Gardelis, C. G. Smith, C. H. W. Barnes, E. H. Linfield, and J. Ritchie, Phys. Rev. B **60**, 7764 (1999).
[77] H. J. Zhu, M. Ramsteiner, H. Kostial, M. Wassermeier, H. P. Schononherr, and K. H. Ploog, Phys. Rev. Lett. **87**, 016601 (2001).
[78] M. Kohda, Y. Ohno, K. Takamura, F. Matsukura, and H. Ohno, Jpn. J. Appl. Phys., Part 2 **40**, L1274 (2001).
[79] H. Breve, S. Nemeth, Z. Liu, J. De Boeck, and G. Borghs, J. Magn. Magn. Mater. **226–230**, 933 (2001).
[80] J. A. Katine, F. J. Albert, R. A. Buhrman, E. D. Myers, and D. C. Ralph, Phys. Rev. Lett. **84**, 3149 (2000).
[81] J. Nitta, T. Ahazaki, H. Takayanngi, and T. Enoki, Phys. Rev. Lett. **78**, 1335 (1997).
[82] R. Buhrman, WTEC Spin Electronics Workshop, Washington, DC, 2 November 2001 (viewgraphs from the presentation are available at http://www.wtec.org/spin/views/buhrman/index.htm).
[83] There are several useful resources available at http://www.wtec.org, from the World Technology (WTEC) study on spin electronics, including ''Spin Electronics: Highlights of Recent US Research and Developments Activities in Spin Electronics'' (http://www.wtec.org/spin_us_summary.pdf) and viewgraphs from the WTEC Workshop on Spin Electronics (http://www.wtec.org/spin/views/index/htm).
[84] T. Dietl, H. Ohno, F. Matsukura, J. Cibert, and D. Ferrand, Science **287**, 1019 (2000).
[85] C. Zener, Phys. Rev. **81**, 440 (1950); **83**, 299 (1950).
[86] See, for example, *Introduction to Nitride Semiconductor Blue Lasers and Light-Emitting Diodes*, edited by S. Nakamura and S. F. Chichibu (Taylor and Francis, London, 2000).
[87] S. Nakamura, S. J. Pearton, and G. Fasol, *The Blue Laser Diode* (Springer, Berlin, 2000).
[88] H. Morkoç, A. Di Carlo, and R. Cingolani, Solid-State Electron. **46**, 157 (2002).
[89] See, for example, the special issue of IEEE Trans. Electron. Devices **48**, 405 (2001), edited by U. K. Mishra and J. C. Zolper.
[90] S. J. Pearton, F. Ren, A. P. Zhang, and K. P. Lee, Mater. Sci. Eng., R. **30**, 55 (2000).
[91] See, for example, H. Morkoç, Mater. Sci. Eng., R. **33**, 135 (2001); *Nitride Semiconductors and Devices* (Springer, Berlin, 1999).

[92] S. J. Pearton, J. C. Zolper, R. J. Shul, and F. Ren, J. Appl. Phys. **86**, 1 (1999).
[93] Some of the data are taken from B. E. Foutz; see http://iiivtn.cornell.edu/www/foutz/nitride.html).
[94] O. Brandt, H. Yang, H. Kostial, and K. H. Ploog, Appl. Phys. Lett. **69**, 2707 (1996).
[95] Y. Zohta, Y. Iwasaki, S. Nakamura, and T. Mukai, Jpn. J. Appl. Phys., Part 2 **40**, L423 (2001).
[96] T. Yamamoto and H. Katayama-Yoshida, Jpn. J. Appl. Phys., Part 2 **36**, L180 (1997).
[97] H. Katayama-Yoshida, R. Kato, and T. Yamamoto, J. Cryst. Growth **231**, 438 (2001).
[98] P. Kozodoy, M. Hansen, S. P. DenBaars, and U. K. Mishra, Appl. Phys. Lett. **74**, 3681 (1999).
[99] I. D. Goepfert, E. F. Schubert, A. Osinsky, P. E. Norris, and N. N. Faleev, J. Appl. Phys. **88**, 2030 (2000).
[100] A. Y. Polyakov, N. B. Smirnov, A. V. Govorkov, A. V. Osinsky, P. E. Norris, S. J. Pearton, J. Van Hove, A. M. Wowchack, and P. P. Chow, J. Appl. Phys. **90**, 4032 (2001).
[101] R. Zeisel, M. W. Bayerl, S. T. B. Goennenwein, R. Dmitrov, O. Ambacher, M. S. Brandt, and M. Stutzmann, Phys. Rev. B **61**, 16283 (2000).
[102] T. L. Tansley, E. M. Goldys, M. Godlewski, B. Zhan, and H. Y. Zou, *GaN and Related Materials*, edited by S. J. Pearton (Gordon and Breach, Amsterdam, 1997), Chap. 8.
[103] C. M. Wolfe, N. Holonyak, Jr., and G. E. Stillman, *Physical Properties of Semiconductors* (Prentice–Hall, Englewood Cliffs, NJ, 1989).
[104] A. R. Hutson, Phys. Rev. **108**, 222 (1957).
[105] D. C. Look, J. W. Hemsky, and J. R. Sizelove, Phys. Rev. Lett. **82**, 2552 (1999).
[106] K. Minegishi, Y. Koiwai, Y. Kikuchi, K. Yano, M. Kasuga, and A. Shimizu, Jpn. J. Appl. Phys., Part 2 **36**, L1453 (1997).
[107] C. Rouleau, S. Kang, and D. Lowndes (unpublished).
[108] T. Yamamoto and H. Katayama-Yoshida, Jpn. J. Appl. Phys., Part 2 **38**, L166 (1999).
[109] M. Joseph, H. Tabata, and T. Kawai, Jpn. J. Appl. Phys., Part 2 **38**, L2505 (1999).
[110] T. Aoki, Y. Hatanaka, and D. C. Look, Appl. Phys. Lett. **76**, 3257 (2000).
[111] Y. R. Ryu, S. Zhu, D. C. Look, J. M. Wrobel, H. M. Jeong, and H. W. White, J. Cryst. Growth **216**, 330 (2000).
[112] J. Blinowski, P. Kacman, and J. A. Majewski, Phys. Rev. B **53**, 9524 (1996).
[113] T. Dietl, H. Ohno, and F. Matsukura, Phys. Rev. B **63**, 195205 (2001).
[114] T. Dietl, J. Cibert, D. Ferrand, and Y. Merle d'Aubigne, Mater. Sci. Eng., B **63**, 103 (1999).
[115] T. Dietl, J. Cibert, D. Ferrand, and Y. Merle d'Aubigne, Phys. Rev. B **55**, 3347 (1997).
[116] T. Dietl, J. Appl. Phys. **89**, 7437 (2001).
[117] K. Nishizawa and O. Sakai, Physica B **281/282**, 468 (2000).
[118] J. Schliemann, J. Konig, and A. H. MacDonald, Phys. Rev. B **64**, 165201 (2001).
[119] J. Schliemann, J. Konig, H. H. Lin, and A. H. MacDonald, Appl. Phys. Lett. **78**, 1550 (2001).
[120] J. Konig, H. H. Lin, and A. H. MacDonald, Phys. Rev. Lett. **84**, 5628 (2000).
[121] T. Jungwirth, W. A. Atkinson, B. H. Lee, and A. H. MacDonald, Phys. Rev. B **59**, 9818 (1999).
[122] B. Lee, T. Jungwirth, and A. H. MacDonald, Phys. Rev. B **61**, 15606 (2000).
[123] T. Dietl, J. Konig, and A. H. MacDonald, Phys. Rev. B **64**, 241201 (2001).
[124] M. Abolfath, T. Jungwirth, J. Brum, and A. H. MacDonald, Phys. Rev. B **63**, 054418 (2001).
[125] J. Konig, T. Jungwirth, and A. H. MacDonald, Phys. Rev. B **64**, 184423 (2001).
[126] V. I. Litvinov and V. K. Dugaev, Phys. Rev. Lett. **86**, 5593 (2001).
[127] M. Berciu and R. N. Bhatt, Phys. Rev. Lett. **87**, 107203 (2001).
[128] M. Berciu and R. N. Bhatt, cond-mat/0111045.
[129] I. Vurgafturman and J. R. Meyer, Phys. Rev. B **64**, 245207 (2001).
[130] J. Fernandez-Rossier and L. J. Sham, Phys. Rev. B **64**, 235323 (2001).
[131] M. von Schilfgaarde and O. N. Myrasov, Phys. Rev. B **63**, 233205 (2001).
[132] C. Y. Fong, V. A. Gubanov, and C. Boekema, J. Electron. Mater. **29**, 1067 (2000).
[133] G. A. Medvedkin, T. Ishibashi, T. Nishi, and K. Hiyata, Jpn. J. Appl. Phys., Part 2 **39**, L949 (2000).
[134] M. L. Reed, M. K. Ritums, H. H. Stadelmaier, M. J. Reed, C. A. Parker, S. M. Bedair, and N. A. El-Masry, Mater. Lett. **51**, 500 (2001).
[135] M. K. Reed, N. A. El-Masry, H. H. Stadelmaier, M. K. Ritums, M. J. Reed, C. A. Parker, J. C. Roberts, and S. M. Bedair, Appl. Phys. Lett. **79**, 3473 (2001).
[136] G. T. Thaler *et al.*, Appl. Phys. Lett. **80**, 3964 (2002).
[137] S. Sonoda, S. Shimizu, T. Sasaki, Y. Yamamoto, and H. Hori, J. Cryst. Growth **237–239**, 1358 (2002).
[138] K. Ueda, H. Takata, and T. Kawai, Appl. Phys. Lett. **79**, 988 (2001).
[139] S. A. Chambers *et al.*, Appl. Phys. Lett. **79**, 3467 (2001).
[140] Y. Matsumoto *et al.*, Science **291**, 854 (2001).
[141] N. Theodoropoulou, A. F. Hebard, M. E. Overberg, C. R. Abernathy, S. J. Pearton, S. N. G. Chu, and R. G. Wilson, Phys. Rev. Lett. **89**, 107203 (2002).
[142] M. E. Overberg *et al.*, Materials Research Society Fall Meeting, Boston, 2001 J. Vac. Sci. Technol. B **20**, 969 (2002).
[143] S. Cho *et al.* Phys. Rev. Lett. **88**, 257203 (2002).
[144] G. A. Medvedkin, K. Hirose, T. Ishibashi, T. Nishi, V. G. Voevodin, and K. Sato, J. Cryst. Growth **236**, 609 (2002).
[145] M. Hashimoto, Y. Z. Zhou, M. Kanamura, and H. Asahi, Solid State Commun. **122**, 37 (2002).
[146] S. Choi, G. B. Cha, S. C. Hong, S. Cho, Y. Kim, J. B. Ketterson, S. Y. Jeong, and G. C. Yi, Solid State Commun. **122**, 165 (2002).
[147] S. J. Pearton *et al.*, J. Appl. Phys. **92**, 2047 (2002).
[148] N. Theodoropoulou, K. P. Lee, M. E. Overberg, S. N. G. Chu, A. F. Hebard, C. R. Abernathy, S. J. Pearton, and R. G. Wilson, J. Nanoscience and Nanotechnol. **1**, 1012 (2001).
[149] N. Theodoropoulou, A. F. Hebard, M. E. Overberg, C. R. Abernathy, S. J. Pearton, S. N. G. Chu, and R. G. Wilson, Appl. Phys. Lett. **78**, 3475 (2001).
[150] N. Theodoropoulou, A. F. Hebard, M. E. Overberg, S. J. Pearton, C. R. Abernathy, S. N. G. Chu, and R. G. Wilson, J. Appl. Phys. **91**, 7499 (2002).
[151] N. Theodoropoulou, M. E. Overberg, S. N. G. Chu, A. F. Hebard, C. R. Abernathy, R. G. Wilson, J. M. Zavada, K. P. Lee, and S. J. Pearton, Phys. Status Solidi B **228**, 337 (2001).
[152] N. Theodoropoulou, A. F. Hebard, S. N. G. Chu, M. E. Overberg, C. R. Abernathy, S. J. Pearton, R. G. Wilson, and J. M. Zavada, Appl. Phys. Lett. **79**, 3452 (2001).
[153] S. J. Pearton, N. Theodoropoulou, M. E. Overberg, C. R. Abernathy, A. F. Hebard, S. N. G. Chu, R. G. Wilson, and J. M. Zavada, Mater. Sci. Eng., B **94**, 159 (1992).
[154] S. J. Pearton *et al.*, J. Vac. Sci. Technol. A **20**, 721 (2002).
[155] K. P. Lee, S. J. Pearton, M. E. Overberg, C. R. Abernathy, R. G. Wilson, S. N. G. Chu, N. Theodoropoulou, A. F. Hebard, and J. M. Zavada, J. Electron. Mater. **31**, 411 (2002).
[156] N. Theodoropoulou, A. F. Hebard, S. N. G. Chu, M. E. Overberg, C. R. Abernathy, S. J. Pearton, R. G. Wilson, and J. M. Zavada, Electrochem. Solid-State Lett. **4**, G119 (2001).
[157] S. J. Pearton, K. P. Lee, M. E. Overberg, C. R. Abernathy, N. Theodoropoulou, A. F. Hebard, R. G. Wilson, S. N. G. Chu, and J. M. Zavada, J. Electron. Mater. **31**, 411 (2002).
[158] N. Theodoropoulou, A. F. Hebard, S. N. G. Chu, M. E. Overberg, C. R. Abernathy, S. J. Pearton, R. G. Wilson, J. M. Zavada, and Y. D. Park, J. Vac. Sci. Technol. A **20**, 579 (2002).
[159] M. E. Overberg, N. Theodoropoulou, S. N. G. Chu, S. J. Pearton, C. R. Abernathy, A. F. Hebard, R. G. Wilson, and J. M. Zavada, Mater. Sci. Eng., B **94**, 14 (2002).
[160] M. E. Overberg, B. P. Gila, C. R. Abernathy, S. J. Pearton, M. A. Theodoropoulou, K. T. McCarthy, S. B. Arnason, and A. F. Hebard, Appl. Phys. Lett. **79**, 3128 (2001).
[161] W. Gebicki, J. Strzeszewski, G. Kamler, T. Szyszko, and S. Podsiadlo, Appl. Phys. Lett. **76**, 3870 (2000).
[162] M. Zajac *et al.*, Appl. Phys. Lett. **78**, 1276 (2001).
[163] M. Zajac, J. Gosk, M. Kaminska, A. Twardowski, T. Szyszko, and S. Podsiadlo, Appl. Phys. Lett. **79**, 2432 (2001).
[164] T. Szyszko *et al.*, J. Cryst. Growth **253**, 631 (2001).
[165] S. Kuwabara, T. Kondo, T. Chikyow, R. Ahmet, and H. Munekata, Jpn. J. Appl. Phys., Part 2 **40**, L724 (2001).
[166] M. E. Overberg, C. R. Abernathy, S. J. Pearton, N. A. Theodoropoulou, K. T. McCarthy, and A. F. Hebard, Appl. Phys. Lett. **79**, 1312 (2001).
[167] Y. L. Soo, G. Kioseogluu, S. Kim, S. Huang, Y. H. Kao, S. Kowabara, S.

Owa, T. Kondo, and H. Munekata, Appl. Phys. Lett. **79**, 3926 (2001).
[168] H. Akinaga, S. Nemeth, J. De Boeck, L. Nistor, H. Bender, G. Borghs, H. Ofuchi, and M. Oshima, Appl. Phys. Lett. **77**, 4377 (2000).
[169] U. Wahl, A. Vantomme, G. Langouche, J. C. Corriera, and L. Peralta, Appl. Phys. Lett. **78**, 3217 (2001).
[170] K. Sato and H. Katayama-Yoshida, Jpn. J. Appl. Phys., Part 2 **39**, L555 (2000).
[171] T. Wakano, N. Fujimura, Y. Morinaga, N. Abe, A. Ashida, and T. Ito, Physica C **10**, 260 (2001).
[172] T. Fukumura, Z. Jin, A. Ohtomo, H. Koinuma, and M. Kawasaki, Appl. Phys. Lett. **75**, 3366 (1999).
[173] H. Tang, H. Berger, P. E. Schmid, and F. Levy, Solid State Commun. **92**, 267 (1994).
[174] M. E. Tobar, J. Krupka, E. N. Ivanov, and R. A. Woode, J. Appl. Phys. **83**, 1604 (1998).
[175] H. Tang, K. Prasad, R. Sanjines, P. E. Schmid, and F. Levy, J. Appl. Phys. **75**, 2042 (1994).
[176] E. Yagi, R. R. Hasiguti, and M. Aono, Phys. Rev. B **54**, 7945 (1996).
[177] J. W. DeFord and O. W. Johnson, J. Appl. Phys. **54**, 889 (1983).
[178] R. Y. Korortiev, J. M. Gregie, and B. W. Wessels, Appl. Phys. Lett. **80**, 1731 (2002).
[179] R. N. Bhatt, M. Berciu, M. D. Kennett, and X. Wan, J. Supercond. **15**, 71 (2002).
[180] P. A. Cox, *Transition Metal Oxides* (Oxford University Press, New York, 1992).
[181] D. S. Ginley and C. Bright, MRS Bull. **25**, 37 (2000).
[182] H. L. Hartnagel, A. L. Dawar, A. K. Jain, and Jagadish, *Semiconducting Transparent Thin Films* (IOP, London, 1995).